Amphiphilic, Regioregular Polythiophenes

Bert de Boer,*,† Paul F. van Hutten, Lahoussine Ouali, Valerie Grayer, and Georges Hadziioannou*,‡

Department of Polymer Chemistry, University of Groningen, Materials Science Centre, Nijenborgh 4, NL-9747 AG, Groningen, The Netherlands

Received September 7, 2001; Revised Manuscript Received June 11, 2002

ABSTRACT: The synthesis, characterization, and solid-state morphology of regioregular, amphiphilic polythiophenes based on 3-dodecyl-3′-(3,6,9,12-tetraoxatridecanyl)-2′,5-bithiophene are described. These polythiophenes form stable monolayers on the water subphase of a Langmuir trough and are transferable (Langmuir−Blodgett deposition) to solid substrates to give highly ordered thin films. Mixing of the amphiphilic, regioregular polythiophenes with a nonconducting poly(ethylene glycol), in a 50/50 weight percent ratio, results in the formation of a semiconducting network of polythiophene in the Langmuir−Blodgett film. The solution-cast films of the amphiphilic, regioregular polythiophenes exhibit liquid-crystalline lamellar mesophases with thermotropic transitions at 0, 60, and 120 °C. These transitions are attributed to the melting of the tetraethylene glycol monomethyl ether side chains, the dodecyl side chains, and the polythiophene backbones, respectively. DSC, X-ray diffraction, and optical microscopy were used to identify the thermotropic transitions. The molecular ordering was investigated with X-ray and electron diffraction. Potentially, the regioregular, amphiphilic polythiophenes are applicable as efficient material in field-effect transistors.

Introduction

Shortly after the first chemical preparations of insoluble, unsubstituted polythiophenes (PT) in 1980 by a metal-catalyzed polycondensation,[1,2] research focused on more soluble PTs. The first substituted polythiophene, poly(3-methylthiophene), was found to be insoluble too,[3,4] but extending the substituents resulted in the first environmentally stable and soluble poly(3-alkylthiophenes) (PATs), which were reported by Elsenbaumer and co-workers.[5] This finding started the quest for novel PATs that are soluble and processable into films, which, after oxidation, can exhibit reasonably high conductivities of 1−5 S/cm. Although the synthesis of poly(3-alkylthiophenes) produces very few 2,4′ linkages, it does not solve the lack of regiochemical control over head-to-tail couplings between adjacent thiophene rings. The dimerization of unsymmetrical substituted 3-alkylthiophenes results in three relative orientations, namely (a) 2,5′ or head-to-tail coupling (HT), (b) 2,2′ or head-to-head coupling (HH), and (c) 5,5′ or tail-to-tail coupling (TT). This leads to a mixture of four chemically distinct triad regioisomers when 3-alkylthiophenes are polymerized, and the product is referred to as regioirregular (RIR) PAT.[6]

Regioregular (RR) or head-to-tail (HT) poly(3-alkylthiophenes) present a low-energy planar conformation, leading to highly conjugated polymers due to the very small torsion angles between substituted thiophene rings. HT-coupled PATs can be obtained by two chemically different methods that use the asymmetric coupling of asymmetric monomers, namely the McCullough method [7] and the Rieke method.[8] The HT-coupled polythiophenes produced by these two methods are spectroscopically not distinguishable and exhibit conductivities up to 1000 S/cm.[9,10] The enhanced conductivity of HT-coupled PATs compared to that of RIR PATs can be attributed to better conjugation (fewer 2,4′ linkages) and higher ordering in the solid state,[11] which are the results of the regiochemical control.[9,10] Because of the regiochemical control, RR PATs exhibit quite different properties compared to their RIR analogies, such as smaller band gaps,[11,12] better molecular ordering, and higher crystallinity in their solid state. Because of the better ordering in the solid state, RR PATs exhibit high intrinsic mobilities (10^{-2} cm^2 (V s)$^{-1}$), and hence, they are frequently used as the semiconducting layer in field-effect transistors (FETs).[13,14] Recently, gate-induced superconductivity at temperatures below ~2.35 K was reported for solution-processed RR poly(3-hexylthiophene) (P3HT) in a field-effect device configuration by Schön et al.[15] The authors attribute the appearance of superconductivity to the self-assembling properties of RR P3HT in the solid state, in which the polymers adopt a preferred orientation with respect to the substrate.[13,15,16] Consequently, mobilities of 0.05−0.1 cm^2 (V s)$^{-1}$ were obtained at room temperature.[16]

Morphological control over large areas, however, is difficult to obtain for RR PATs by conventional casting techniques like drop- and spin-casting. Optoelectronic properties such as photo- and electroluminescence, conductivity, and nonlinear optical response[17] are intimately connected to the structure of the polymeric assemblies that constitute the material. Therefore, controlling the assembly process is essential for the preparation of thin film devices with reproducible optoelectronic properties. The Langmuir−Blodgett (LB) technique can provide such control of the assembly process.[18−21] LB techniques offer a unique approach to preparing ordered ultrathin films with well-defined architectures, thus providing a promising and versatile method for constructing molecular devices. Applying the LB technique to conjugated polymers has produced a

---

† Present address: Bell Laboratories, Lucent Technologies, 600 Mountain Avenue, Room 1A-230, Murray Hill, NJ 07974.

‡ Permanent address: Ecole Européenne Chimie Polymères Matériaux (ECPM), Université Louis Pasteur Strasbourg, 25, rue Becquerel, F-67087 Strasbourg Cedex 2, France.

* To whom correspondence should be addressed: e-mail hadzii@ecpm.u-strasbg.fr or bdeboer@lucent.com.

10.1021/ma011591w CCC: $22.00

variety of optoelectronic devices, such as LEDs[22] and FETs.[18] In general, RR PATs used for preparing these devices are based on polythiophenes containing hydrophobic side chains. Spreading these polymers on the air–water interface of a Langmuir trough results in bending of the side chains, which, in turn, cause the thiophene rings to twist away from the coplanar conformation. The benefits of using head-to-tail coupled PATs will be negligible in that case.

Amphiphilic conjugated polymers, however, can be easily processed by the LB technique, resulting in self-assembled, highly oriented monolayers that can be transferred to solid supports for further characterization. The key to obtaining highly oriented films with good conductive properties lies with the design and synthesis of regioregular, amphiphilic polythiophene copolymers with perfectly alternating hydrophobic and hydrophilic side groups that form highly ordered PT films. McCullough and co-workers synthesized these alternating, amphiphilic, and regioregular polythiophenes.[19] Their method relied on the synthesis of an amphiphilic bithiophene that could be selectively functionalized at the 2 and 5′ positions. By coupling of the asymmetric bithiophenes, highly regioregular polythiophenes were obtained, and this method proved to be compatible with various functional side chains. For these reasons, we adapted their method (Supporting Information), and the Experimental Section describes the synthesis of the alternating, amphiphilic, HT-coupled polythiophenes. The obtained RR, amphiphilic PTs were found to give stable LB films that were transferable to solid substrates. Casting from solution onto substrates and subsequent annealing resulted in crystalline films, which were characterized by differential scanning calorimetry (DSC), optical and electron microscopy techniques, and X-ray and electron diffraction. Combined, the characterization techniques revealed a highly ordered, lamellar-like solid-state structure.

Experimental Section

Measurements. ^{1}H NMR spectra were recorded on a Varian Gemini-300 spectrometer with internal lock on the ^{2}H signal of the solvent. Absorbance spectra were measured with a SLM Aminco 3000 diode array spectrometer with UV-grade solvents. Photoluminescence spectra were recorded on a Perkin-Elmer LS50-B spectrofluorimeter with an excitation wavelength at the absorption maximum. The GPC-LS measurements were done in THF using PL-gel mixed-C columns in a Waters Powerline 600 LC-system, equipped with a Waters 996 photodiode detector and a Wyatt Dawn DSP light scattering detector. GPC in chloroform was performed on Spectra Physics AS 1000 coupled with a Shodex RI-71 refractive index detector and a Viskotek H-502 viscometer, and molecular weights were determined relative to polystyrene standards or calculated with a measured d*n*/d*c*. d*n*/d*c* measurements were performed on a Jenoptik Jena interferometer LI-3 in $CHCl_3$ and THF (both HPLC grade) at 25 °C. Matrix-assisted laser desorption/ionization time-of-flight (MALDI–TOF) mass spectra were recorded on a Micromass TofSpec SE spectrometer. All spectra were recorded in the linear mode, in which samples were irradiated under high vacuum using a nitrogen laser (wavelength 337 nm, 4 ns pulse), where each pulse has an energy of 180 μJ. The accelerating voltage and pulse voltage were 20 kV and 2 kV, respectively. Dithranol was used as a matrix, and both matrix and polymer were dissolved in chloroform, mixed (molar ratio 2000:1) and drop-cast (2 μL) on a stainless steel target. Average molecular weights (M_n, M_w) were calculated from the MALDI–TOF data.

Langmuir–Blodgett experiments were performed on computer-controlled Lauda Filmbalance (FW2), with a surface pressure accuracy of 0.05 mN/m. The monolayer properties were studied by measuring surface pressure–area isotherms. LB films were deposited under constant lateral pressure (ranging from 1 to 15 mN/m) on silicon, mica, or quartz substrates. These films were dried and examined by atomic force microscopy (AFM) using a Digital Nanoscope III. Silicon cantilevers were used to acquire topography images in tapping mode at room temperature in ambient conditions. Differential scanning calorimetry analyses were obtained using a Perkin-Elmer DSC-7 that was calibrated with indium. Transmission electron microscopy images were recorded on a JEOL 1200 EX electron microscope operating at 100 kV. X-ray diffraction was performed on an Inel CPS-120 using a glass capillary of 1 mm. An Enraf Nonius FR590 X-ray generator was used producing X-rays with a wavelength of 154 pm (Cu Kα). The X-ray data were corrected for glass. Optical microscopy images were taken on a Zeiss Axiophot microscope equipped with a high-resolution CCD camera (Sony DKC 5000), which was connected to a frame grabber and a personal computer for image processing.

Materials and Methods. The detailed synthesis and characterization of bifunctional, amphiphilic bithiophene (**3**) are described in the Supporting Information. Chemicals were used as received, unless noted otherwise. Water was purified by the Milli-Q filtration system to obtain a resistivity as high as 18.2 MΩ·cm. Chloroform used in LB experiments and spectroscopic analysis was of spectroscopic quality (Uvasol).

Regioregular Polymerization of Amphiphilic Monomer 3 (4, Regioregular DTOT-PT). 2′-Bromo-3′-dodecyl-3-(3,6,9,12-tetraoxatridecanyl)-5-trimethylstannyl-2–5′-bithiophene (**3**) (2.07 g, 2.7 mmol), $Pd(PPh_3)_4$ (0.16 g, 5 mol %), and CuO (0.22 g, 2.7 mmol) were dissolved in 75 mL of DMF and stirred at 110 °C for 21 h. The solution was cooled to room temperature and precipitated in 1 L of methanol. The collected residue was extracted consecutively in a Soxhlet apparatus with methanol, hexane, and chloroform. The hexane fraction contained 580 mg of relatively high molecular weight amphiphilic, regioregular polythiophene DTOT-PT (hex) (M_n = 41 000 g/mol) and the chloroform extraction resulting in 140 mg of high molecular weight amphiphilic, regioregular polythiophene DTOT-PT ($CHCl_3$) (M_n = 54 300 g/mol). ^{1}H NMR spectra of both polymers are identical.

^{1}H NMR ($CDCl_3$): δ (ppm) = 0.80 (t, 3H, CH_3), 1.2 (m, 18H, CH_2), 1.6 (br t, 2H, T–CH_2–CH_2–R (D)), 2.7 (br t, 2H, T–CH_2–R (D)), 3.0 (br t, 2H, T–CH_2–CH_2 (TOT)), 3.3 (s, 3H, OCH_3), 3.4–3.7 (m, 14H, CH_2–O), 6.95 (s, 1H, C=HC (4′, D)), 6.98 (s, 1H, C=CH (4, TOT)).

Polymerization of 3-(3,6,9,12-Tetraoxatridecanyl)-3′-dodecyl-2,5′-bithiophene with Ferric Chloride (Regioirregular DTOT-PT). $FeCl_3$ (1.24 g, 7.63 mmol) and 3-(3,6,9,-12-tetraoxatridecanyl)-3′-dodecyl-2,5′-bithiophene (**1**) (see Supporting Information) (1.0 g, 1.91 mmol) were added to 15 mL of chloroform. The mixture was stirred for 24 h at room temperature, after which the solution was poured out into 750 mL of methanol. The precipitate was collected and extracted with a Soxhlet apparatus for 72 h with methanol, and the product was collected by extraction with chloroform. The chloroform solution was concentrated and precipitated in 1 L of methanol. The collected product yielded 0.42 g of RIR DTOT-PT.

^{1}H NMR ($CDCl_3$): δ (ppm) = 0.80 (t, 3H, CH_3), 1.2 (m, 18H, CH_2), 1.6 (br t, 2H, T–CH_2–CH_2–R (D)), 2.7 (br t, 2H, T–CH_2–R (D)), 3.0 (br t, 2H, T–CH_2–CH_2 (TOT)), 3.3 (s, 3H, OCH_3), 3.4–3.7 (m, 14H, CH_2–O), 6.95 (s, 1H, C=HC (4′, D)), 6.98 (s, 1H, C=CH (4, TOT)), shoulder at 7.01, 7.06 and 7.12–7.14 (br ds, 2H, CHs of thiophenes due to regioirregular coupling).

Results and Discussion

Synthesis and Characterization of Amphiphilic, Head-to-Tail Polythiophenes. The synthesis of amphiphilic, head-to-tail coupled bithiophenes, based on methods previously developed by McCullough,[19,23] is described in the Supporting Information. The design is

Scheme 1. Synthesis of Amphiphilic Monomer 2′-Bromo-3′-dodecyl-3-(3,6,9,12-tetraoxatridecanyl)-5-trimethylstannyl-2−5′-bithiophene (3) and Its Polymerization To Yield Regioregular, Amphiphilic Polythiophenes (4): (a) NBS in Chloroform/Acetic Acid (50/50); (b) 1, LDA, THF, −78 °C; 2, Me$_3$SnCl; (c) Pd(PPh$_3$)$_4$, CuO, DMF, 110 °C

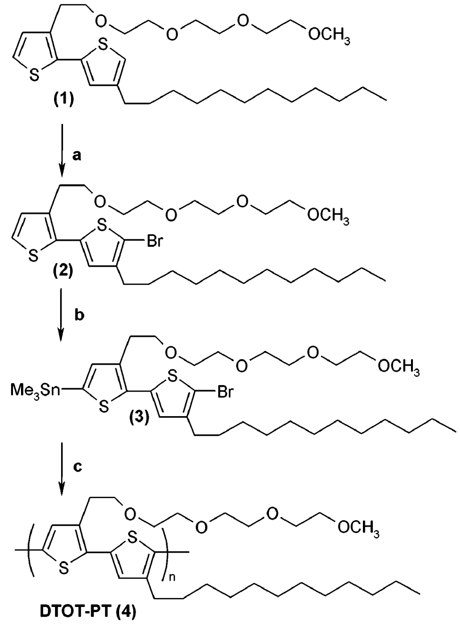

based on the synthesis of two distinct monomers bearing a hydrophilic tetraethylene glycol side chain and a hydrophobic dodecyl side chain. The thiophene monomer containing tetraethylene glycol side chains was designed and synthesized because its length is comparable to the dodecyl side chain of the hydrophobic, 3-dodecylthiophene monomer, which, in turn, was synthesized for its tendency to form ordered mesophases in the solid state.[9,24] Coupling[25] of both monomers resulted in an amphiphilic, head-to-tail coupled dimer (**1**). As depicted in Scheme 1, the amphiphilic dimer was first selectively brominated at its 2-position (**2**) and subsequently converted into a bifunctional (2,5′) monomer (**3**) capable of undergoing a poly-Stille-coupling, resulting in an alternating, amphiphilic, RR polythiophene (DTOT-PT) (**4**).

After the polymerization, the product was precipitated in methanol, and a Soxhlet extraction was performed with methanol, hexane, and chloroform. The methanol fraction of the Soxhlet extraction contained only very low molecular weight oligomers that were not used for further characterization. The hexane fraction contained regioregular, amphiphilic polythiophene with 78 repeat units of the dimer (M_n = 41 000 g/mol), as determined by gel permeation chromatography coupled with light scattering (GPC-LS) in chloroform, whereas the chloroform extract yielded the highest molecular weight fraction of 104 repeat units of dimer (M_n = 54 300 g/mol). Both polymers possess very low polydispersities (*D*). The results are summarized in Table 1. The overall yield for the amphiphilic RR PTs starting from 3-bromothiophene and 2-(3-thienyl)ethanol is 4.5%.

From ^{1}H NMR data, the percentage of head-to-tail coupled polythiophene was calculated to be >95% for both polymers. The resonances of the non-head-to-tail coupled dimers should be quite distinct from the head-to-tail coupled ones.[6] For comparison, monomer **1** was also polymerized with ferric chloride (FeCl$_3$), which resulted in regioirregular (RIR) amphiphilic polythiophene. From ^{1}H NMR data, the random coupling of the dimer is clearly observed. Additional resonances can be observed around δ = 7.12−7.14, 7.06 and a clear shoulder at 7.01, which are indicative of the three different triads in RIR PATs.[6] The ^{1}H NMR spectrum of RIR PT indicated that ca. 25% of the dimers in the polythiophene backbone were non-HT-coupled.

Table 1. Molecular Weights and Properties of Alternating, Amphiphilic, RR Polythiophenes after Soxhlet Extraction with Hexane and Chloroform and Amphiphilic, RIR Polythiophene Obtained by Polymerization with FeCl$_3$

	DTOT-PT (RR, hex) chloroform/THF	DTOT-PT (RR, CHCl$_3$) chloroform/THF	DTOT-PT (RIR) THF
M_w (g mol^{-1})[a]	44 300/20 000	55 900/32 200	32 200
M_n (g mol^{-1})[a]	41 000/15 900	54 300/27 700	19 700
N (rep units)[a]	78/30	104/53	38
D (=M_w/M_n)[a]	1.08/1.26	1.03/1.16	1.63
d*n*/d*c* (mL g^{-1})[a]	0.148/0.171	0.155/0.141	0.179
d*n*/d*c* (mL g^{-1})[b]	0.116/0.121	0.118/0.127	0.119
M_w (g mol^{-1})[b]	72 300/28 000	96 700/35 700	48 300
M_n (g mol^{-1})[b]	66 800/22 600	93 800/30 800	29 600
N (rep units)[b]	128/43	180/59	57
D (=M_w/M_n)[b]	1.08/1.26	1.03/1.16	1.63
M_n (g mol^{-1})[c]	3750	4675	4800
M_w (g mol^{-1})[c]	4150	5380	5500
D (=M_w/M_n)[c]	1.11	1.15	1.15
HT coupling (%)	>95	>95	∼75
λ_{max} (nm)	433	440	433
PL$_{max}$ (nm)	574	586	567

[a] Determined by GPC-LS in CHCl$_3$ or THF assuming 100% mass recovery. [b] d*n*/d*c* measured in CHCl$_3$ or THF. Molecular weights determined by GPC-LS using the measured d*n*/d*c*. [c] Determined by MALDI−TOF MS.

Although GPC-LS demonstrates high molecular weights for the amphiphilic, RR polythiophenes (Table 1), one has to take into account that GPC-LS measurements are normally used for coillike polymers (like polystyrene), which have a smaller hydrodynamic volume than the rodlike polythiophenes. Molecular weight values measured by GPC-LS in THF demonstrate that the amphiphilic polythiophenes exhibit a much lower hydrodynamic volume, indicating a more compact conformation in THF than in chloroform. Most probably, the less stretched chain conformation (decreased hydrodynamic volume) is more comparable to the hydrodynamic volume of coillike polymers, and therefore, the molecular weights determined in THF are more representative of the actual molecular weights of the polythiophenes. In general, molecular weight analysis of rigid-rod polymers by GPC-LS results in overestimated molecular weights.[26] For poly(3-hexylthiophene)s measured with GPC-LS using polystyrene calibration standards, both the number- and weight-averaged molecular weights are overestimated by factors of 2.0.[27]

When the molecular weights are determined by light scattering using the refractive index increment (d*n*/d*c*) that was measured with an interferometer, even higher values are obtained. When this method is used, the difference between the molecular weights measured in chloroform and in THF becomes larger. This difference might arise from the light source of the interferometer used for the determination of d*n*/d*c*. The interferometer uses white light to determine the refractive index increment, which is partially absorbed by the polythiophene solutions, resulting in an inaccurate value of d*n*/d*c*.

Matrix-assisted laser desorption/ionization time-of-flight (MALDI−TOF) mass spectroscopy resulted in the

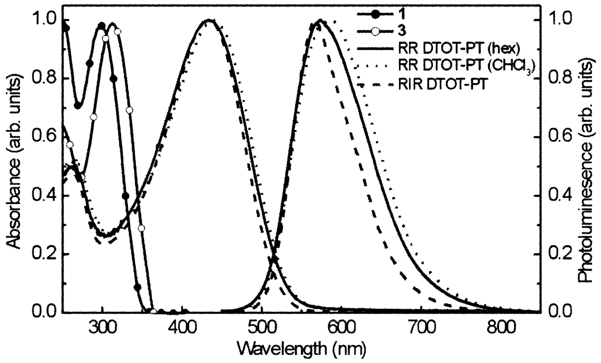

Figure 1. UV−vis spectra of amphiphilic bithiophene (**1**) and functionalized bithiophene monomers (**3**) and UV−vis and photoluminescence spectra of RR polythiophenes and RIR polythiophene.

detection of very low molecular weights. Unfortunately, MALDI−TOF is less reliable, because of the mass dependence of the desorption/ionization process and the mass-dependent detection efficiency in MALDI−TOF. Because of this, the higher molar mass components tend to be underrepresented with respect to the lower mass components.[28] On the other hand, previous literature reports already demonstrated overestimated molecular weights of monodisperse oligothiophenes by a factor of 2 when determination by GPC is compared to MALDI−TOF.[29]

Two independent and accurate methods can be used to determine the molecular weights of polymers. One is GPC-LS calibrated with well-defined oligomers of identical composition as the polymer. This was demonstrated in ref 26 for rigid-rod polymers based on tetrahydropyrene. This method requires the tedious, stepwise synthesis of oligomers, which is not the goal of this work. The other method is based on using the Mark−Houwink equation, for which the intrinsic viscosity is required.[27] Unfortunately, the amphiphilic polythiophenes exhibited intrinsic viscosities too low to make an accurate estimation of the Mark−Houwink constants.

The molecular weight of RIR DTOT-PT is comparable to that of RR DTOT-PT ($CHCl_3$), but the RIR polymer possesses a higher polydispersity, due to the polymerization with $FeCl_3$. Moreover, this polymer was not purified by Soxhlet extraction with various solvents, a procedure that would result in fractionation of the polymer and a narrower molecular weight distribution.

The UV−vis and photoluminescence spectra of the dimer, the 2,5′-functional dimer, and the amphiphilic polymers in chloroform clearly demonstrate the decreasing optical band gap with increasing molecular weights (Figure 1). Whereas the dimers show absorption in the UV range, the polymers possess relatively high wavelength absorption maxima (λ_{max}) and photoluminescence maxima (PL_{max}), indicating the increase in conjugation length (reduction of the optical band gap). Also, the difference between the hexane-extracted polymer and the chloroform-extracted polymer is obvious from the absorption and fluorescence spectra, indicating that the latter contains the higher molecular weight fraction with a higher conjugation length.

Although the molecular weight of the regioirregular amphiphilic polythiophene is determined to be higher than that of RR DTOT-PT (hex) and comparable to that of RR DTOT-PT ($CHCl_3$) by all methods described above, it demonstrates roughly the same absorption spectrum as RR DTOT-PT (hex), which is indicative of the nonperfect head-to-tail coupling. Because of head-to-head or tail-to-tail coupling, the thiophene rings in the polymer are forced into a nonplanar conformation, leading to poorer π-orbital overlap and, therefore, an increasing optical band gap. This is even more pronounced in the photoluminescence, where the nonplanar conformation induces photoluminescence of higher energy, due to higher positioned excited states. Therefore, the photoluminescence will be blue-shifted compared to RR DTOT-PT with the same or even lower molecular weight.

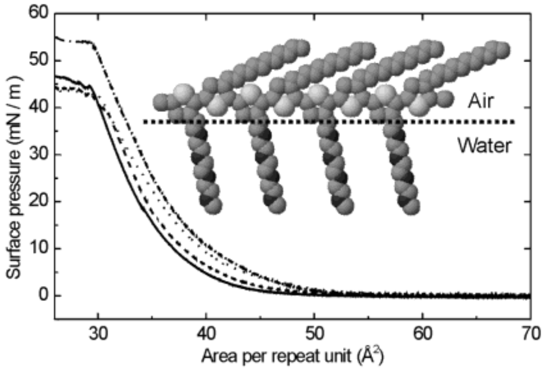

Figure 2. Surface pressure−area isotherms of RR DTOT-PT (hex) spread at a water subphase temperature of 30 °C at a concentration of 0.169 (—) and 0.085 mg/mL (· · ·) in chloroform and at a subphase temperature of 60 °C at a concentration of 0.169 (− − −) and 0.085 mg/mL (− · −). Inset: space-filling model of the amphiphilic, RR polythiophene at the water−air interface. Black: oxygen; light gray: sulfur; gray: carbon.

The spectroscopic studies demonstrate the advantages of head-to-tail coupled polythiophenes with respect to the control of the conformation. Even though the molecular weight of RR DTOT-PT ($CHCl_3$) is comparable to that of RIR DTOT-PT, the regioregular PT possesses a photoluminescence maximum that is almost 20 nm red-shifted. Ultimately, regiochemical control will give rise to improved optoelectronic properties of polythiophenes.[14−16]

Structural and Spectroscopic Properties from Langmuir−Blodgett Films of Regioregular, Amphiphilic Polythiophene and Their Blends with Poly(ethylene glycol). Langmuir−Blodgett Films of Regioregular, Amphiphilic Polythiophene as the Sole Component. The formation of uniform films of RR DTOT-PT at the air−water interface is very sensitive to the preparation conditions such as temperature, solvent, and concentration. At too high a concentration, the films, spread from chloroform solution, rapidly became inhomogeneous, indicating aggregation of the rigid polythiophenes. To avoid aggregation already in solution, RR DTOT-PT (hex) was used in these experiments, because of its better solubility in chloroform. Chloroform solutions of this RR PT spread readily onto the water surface of the Langmuir trough. The amphiphilic nature of this kind of PT ensures that the tetraethylene glycol groups go into the water while the long alkyl chains stick up into the air.[19,21] The design of alternating hydrophilic and hydrophobic substituents results in a preorganization of the polymer on the water subphase, which allows full conjugation of the π-electrons due to the coplanar configuration of neighboring thiophene units, as schematically depicted in Figure 2 (inset).

Figure 2 also shows the surface pressure−area isotherms of films of RR DTOT-PT (hex), spread from chloroform at different concentrations and compressed at two distinct subphase temperatures. The total compression time was kept constant at 60 min. Although films spread at higher concentration demonstrated a higher compressibility, these films also frequently collapsed before reaching the highly condensed state (>30 mN/m). The isotherms recorded at elevated temperatures of the subphase demonstrate a lower compressibility and a more rapid transition from the expanded to the condensed state, suggesting a larger occupied area per repeat unit due to thermal motion. All pressure−area isotherms lead to a close-packed monolayer and reveal a collapse of this layer at ∼29 Å^2 per polythiophene repeat unit, which agrees with the calculated area of a dimer estimated from X-ray diffraction data (section: Solid-state properties of amphiphilic, regioregular polythiophenes; ∼30 Å^2)[23] and with previously reported LB data on similar compounds.[19,20] Beyond the collapse point (area per repeat unit <29 Å^2), these amphiphilic RR PTs have been reported to form bundles of PTs or tubular superstructures (nanowires) with dimensions of ∼60 nm wide, 10−15 nm high, and a length of several microns.[30] X-ray diffraction experiments showed that the wires were less ordered than the monolayer from which they were formed. Exposing the nanowires to iodine vapor resulted in a conductivity of 40 S/cm.[30]

In a stabilization experiment, a film spread at 0.169 mg/mL (chloroform) and compressed to a surface pressure (Π) of 15 mN/m at 20 °C proved to be stable for a long period of time (at least 1000 min), enabling the transfer of mono- or multilayers of RR DTOT-PT (hex) onto solid substrates. Transfer of the film allows the evaluation of its morphology by imaging techniques, e.g., AFM. Figure 3 shows the surface pressure−area isotherm of a film of RR DTOT-PT (hex) at 20 °C. Films were transferred by vertical deposition onto mica at three different surface pressures as indicated in Figure 3 (A: $\Pi = 1.5$ mN/m, B: $\Pi = 5.0$ mN/m; C: $\Pi = 15$ mN/m). The film transfer to mica occurred smoothly without rupture of the LB film and with a transfer ratio of unity. AFM of LB films transferred at three distinct surface pressures reveals that the RR DTOT-PT aggregates into wormlike clusters with a height around 2 nm and a length of several tens of nanometers (Figure 3). The contour length of the 78-unit polymer chain (determined by GPC in $CHCl_3$) would be 58 nm. The packing density gradually increases with pressure. The surface roughness initially remains within 2 nm, implying that the molecules have their long axis parallel to the film surface. At 15 mN/m, the film surface shows protrusions at least 5 nm high in some places, indicating that some aggregates have been pushed out of the first layer and forced to point upward or to pile up.

Many tens of layers can be deposited onto quartz by repeated vertical dipping in the LB trough at a surface pressure of 8.0 mN/m. The increase of the number of layers on the substrate is indicated by an increase of the optical density (Figure 4 inset). Optical absorption (Figure 4) is red-shifted relative to the solution and peaks at 445 nm for 30 layers and at 455 nm for 60 layers. The fluorescence spectra of the multilayers are much narrower than those of the solution and more red-shifted than the absorption spectra. The fluorescence shifts to the blue upon increasing the number of layers (maximum at 634 nm for 30 layers and at 618 nm for 60 layers). The narrowing of the spectra and the

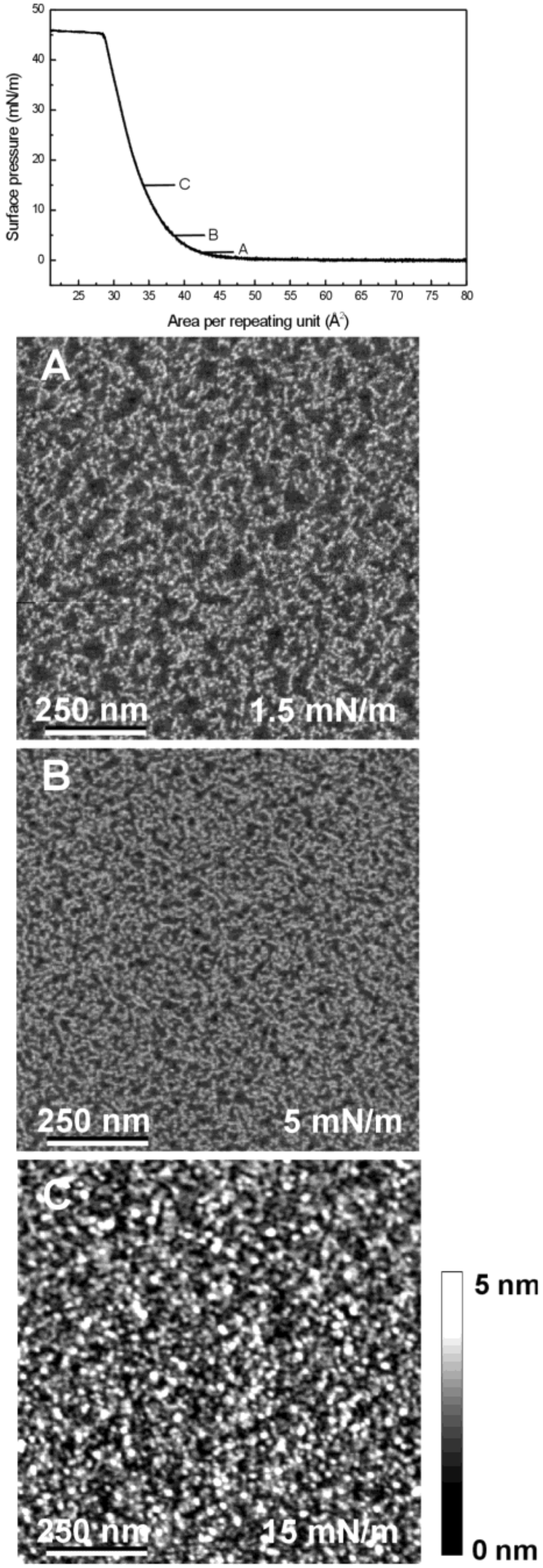

Figure 3. Surface pressure−area isotherm of RR DTOT-PT (hex) at 20 °C and spread from a chloroform solution of 0.169 mg/mL. Points A, B, and C mark the surface pressures at which films were transferred onto mica. AFM-tapping mode images of the LB films transferred onto mica at 1.5 (A), 5 (B), and 15 mN/m (C).

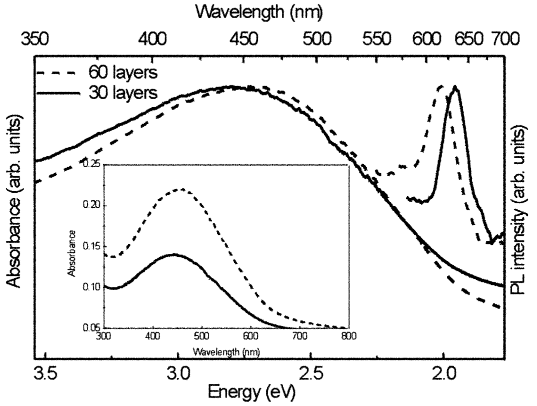

Figure 4. Normalized absorption and photoluminescence spectra of 30 and 60 layers of RR DTOT-PT transferred onto quartz at a surface pressure of 8.0 mN/m. Inset: absolute absorption spectra of 30 and 60 deposited layers.

dependence on the number of layers suggest three-dimensional order, with full orientational correlations between the layers, in the multilayer.

Langmuir–Blodgett Films of Mixtures of Regioregular, Amphiphilic Polythiophenes and Poly(ethylene glycol). In the quest for transparent and flexible electrodes, Cao et al. mixed camphorsulfonic acid-doped polyaniline (PANI–CSA) with poly(methyl methacrylate) (PMMA)[31–33] or polyethylene[31] and reached electrical conductivities of 1 S/cm in polyblends containing PMMA and only 2 wt % PANI–CSA. Transmission electron microscopy studies demonstrated that an interconnected network was formed upon the addition of more than 1 wt % PANI–CSA to PMMA.[33] In analogy with the blending and solution processing of PANI–CSA and PMMA, we mixed RR DTOT-PT with poly(ethylene glycol) (PEG) in order to achieve a percolated system in thin LB films. PEG was used for its compatibility with the tetraethylene glycol monomethyl ether side chains of the RR PT. The polymer mixtures (RR DTOT-PT (hex), PEG M_n=10 000 g/mol) were dissolved in chloroform with a concentration of 0.1 mg/mL and spread on the water subphase. The isotherms were recorded at 20 °C with a barrier speed of 30 cm^2/min (Figure 5). LB films were deposited under constant lateral pressure (6–6.5 mN/m) onto silicon substrates. The inset in Figure 5 shows a magnification of the low-area range of the isotherms.

Although PEG dissolves in water, it remains on the water surface when initially deposited as a solution in chloroform. This finding is explained as an effect of the surface tension. Compression of the Langmuir layer leads to dissolution of the PEG at some point, while the pressure is expected to remain essentially constant during this process. In Figure 5, the surface pressure is plotted as a function of the area per repeat unit of amphiphilic PT, and the isotherms are normalized to the amount of PT introduced. The isotherms demonstrate a higher compressibility of the films for lower PT content, indicating that the rigid polythiophenes have a strong influence on the compressibility of the film. As described above, films of pure amphiphilic PTs exhibit an area per repeat unit of 29 Å^2. This is reflected in the isotherms of the mixtures as a steady increase of the surface pressure during compression of these films up to a value around 8.5 mN/m, where the surface area has reached a value of ca. 35 Å^2, for both mixtures. Hence, it was concluded that the PEG has dissolved into the water phase at this point and that only amphiphilic PT forms the monolayer film.

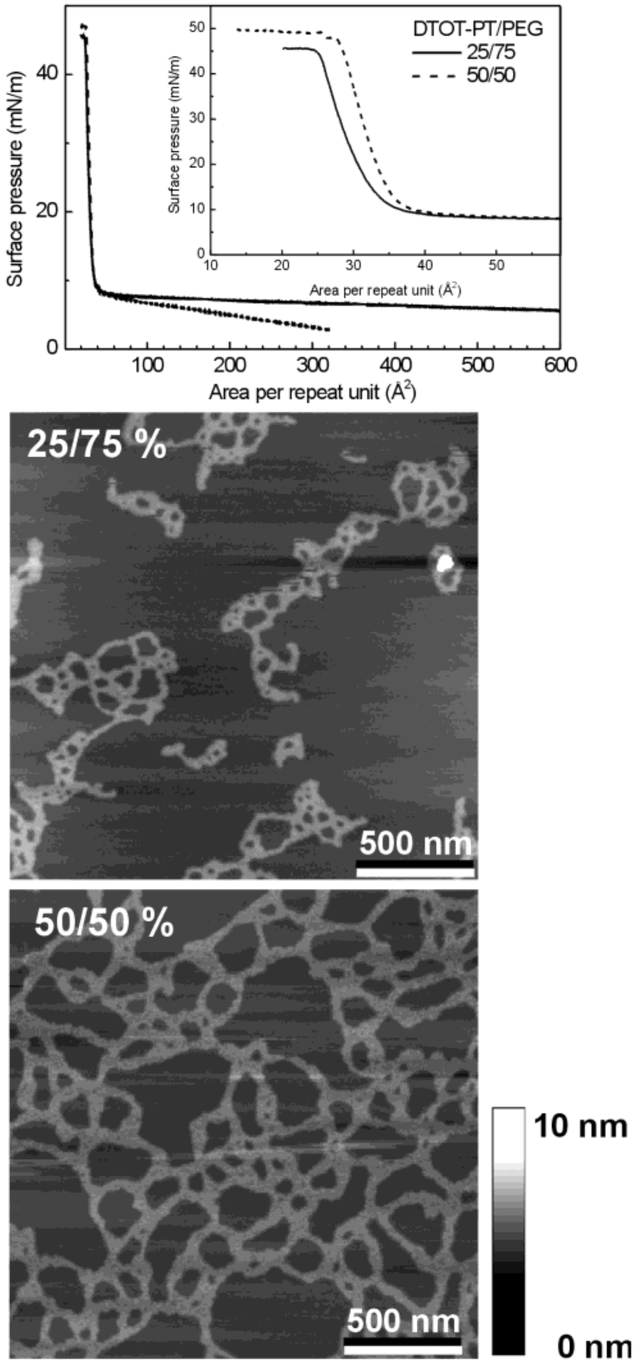

Figure 5. Surface pressure–area isotherms of mixtures of RR DTOT-PT and PEG on the water subphase and AFM images of the films transferred at a surface pressure of 6–6.5 mN/m.

At a surface pressure of 6–6.5 mN/m, approximately half of the initial amount of PEG will still be present on the water. At this pressure, films were transferred onto silicon substrates. Evaluation of the thin-film morphology by AFM shows that a continuous network of conducting polymer can be formed by mixing 50 wt % of amphiphilic PT (bright) together with PEG (dark). Diluting the mixture with more PEG (25/75) results in discontinuities of the PT phase and a smaller apparent thickness of the continuous path. The PT threads envelop areas of the PEG phase, which is therefore disperse. The PEG areas vary greatly in size: many are an order of magnitude larger than the thread diameter. Closer inspection, however, reveals the presence of very small PEG areas. The width and height of the threads formed by PT are quite uniform over the whole film (50–100 and ~2 nm, respectively). This resembles the wormlike aggregates found in films that consist solely of RR DTOT-PT (Figure 3). Probably, the wormlike aggregates have the tendency to form their own domains (like-likes-like) in films of mixtures of polymers. This is interpreted as the PT being oriented perpendicular to the thread axis, whereby the molecular length of ca. 60 nm for the amphiphilic PT used here sets the diameter of the threads. Normally polymer blends tend to macrophase separate into domains with typical length scales of micrometers due to this principle of preferred interaction with their own species (minimizing the interfacial tension). By using a mixture of regioregular, amphiphilic polythiophene and poly(ethylene glycol), we obtained percolated systems with path widths of tens of nanometers. By adjusting the amount of polythiophene and the surface pressure of the LB trough, one can control the percolation.

Solid-State Properties of Amphiphilic, Regioregular Polythiophenes. Because of the confined space in LB films (monolayers), certain properties of polymers, e.g., macrophase separation, thermotropic and lyotropic behavior, can change or even vanish upon going from the bulk, condensed state to the monolayer. Data obtained from macroscopic measurements should, therefore, be carefully compared with those of ultrathin films obtained by LB techniques. In this section, the bulk solid-state properties of amphiphilic, RR PTs are investigated by means of differential scanning calorimetry (DSC), X-ray and electron diffraction, optical microscopy, and transmission electron microscopy (TEM).

Polymers consisting of long side chains connected to a rigid backbone are often referred to as hairy rod polymers. These polymers are known to exhibit thermotropic behavior with liquid-crystalline mesophases.[9,34−37] The amphiphilic, regioregular polythiophenes described above belong to this class and exhibit interesting thermotropic transitions.

DSC analysis of RR DTOT-PT (hex) reveals three clear thermotropic transitions upon cooling from the isotropic melt at 200 °C down to −50 °C at 10 °C/min: a sharp transition at 85 °C ($\Delta H = -4$ J/g) and two less pronounced transitions at 55 °C ($\Delta H = -2$ J/g) and 5 °C ($\Delta H = -2$ J/g). The subsequent heating scan gives rise to the corresponding endothermic transitions at 5 °C ($\Delta H = 1$ J/g), 60 °C ($\Delta H = 11$ J/g), and 120 °C ($\Delta H = 3$ J/g). The transition around 5 °C is attributed to melting (crystallization) of the tetraethylene glycol monomethyl ether side chains, and the transition at 60 °C is attributed to the melting (crystallization) of the dodecyl side chains.[38] The third transition (120 °C) results from melting of the thiophene backbones. Upon cooling from the isotropic melt, the backbone crystallization requires a strong undercooling.

The high molecular weight amphiphilic polythiophene RR DTOT-PT ($CHCl_3$) exhibits similar thermotropic transitions, but at slightly different temperatures (down-scan: 100 °C, $\Delta H = -7$ J/g; 55 °C, $\Delta H = -2$ J/g; 0 °C, $\Delta H = -3$ J/g; up-scan: 5 °C ($\Delta H = 1$ J/g); 60 °C, $\Delta H = 2$ J/g; 130 °C, $\Delta H = 5$ J/g). Upon heating, the higher molecular weight PT demonstrates the same melting temperature of the dodecyl side chains and a slightly higher melting temperature of the PT backbone, as expected.

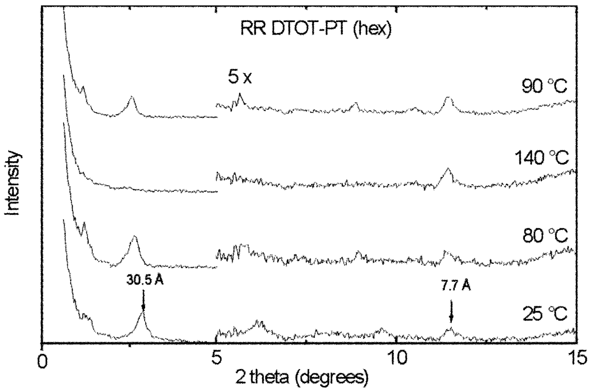

Figure 6. X-ray diffraction of RR DTOT-PT (hex) at distinct temperatures in a glass capillary, successively measured on the same sample (from bottom to top).

Similar to the regioregular polythiophenes, the regioirregular, amphiphilic polythiophene exhibits two melting transitions upon heating that are attributed to side-chain melting, at 0 °C ($\Delta H = 2$ J/g) and at 65 °C ($\Delta H = 11$ J/g). The latter consists of multiple endothermic transitions, resulting in a huge, broad transition with multiple peaks and large endothermic energy. Therefore, this transition is attributed not only to the melting of the dodecyl side chains but also to the melting of the polythiophene backbone. Furthermore, a very small peak is observed at 95 °C, which is also attributed to the melting of the polythiophene backbone. The reverse scan, on the other hand, reveals a small exothermic crystallization at 65 °C (crystallization of the polythiophene backbone, $\Delta H = -1$ J/g) and a large, broad transition centered around 5 °C with an onset at 30 °C ($\Delta H = -10$ J/g). This implies crystallization of the dodecyl and the tetraethylene glycol side chains in that temperature range, resulting from nonperfect ordering in the solid state due to the regioirregular coupling of the bithiophene repeat units.

Evaluation of the bulk morphology by X-ray diffraction is a powerful method to resolve the lattice spacing of ordered films of RR PTs.[9,20,36,38,39] This technique also demonstrated that RIR PATs and unsubstituted PTs were totally amorphous.[9] For our RR DTOT-PT, Figure 6 clearly shows the (200) Bragg reflection at 2 Å = 2.9°, corresponding to a *d*-spacing of 30.5 Å at 25 °C. The distance of 30.5 Å reflects the spacing between polythiophenes separated by two side chains. The polythiophene chains will order themselves in alternating orientation, favoring hydrophilic and hydrophobic interactions. The ordered structured is schematically depicted in Figure 7. Overlap (interdigitation) between side chains in neighboring stacks is minimal although there can be ordering of the side chains across the layer–layer interface.[36] STM imaging of two-dimensional crystals of RR poly(3-dodecylthiophene) on highly oriented pyrolytic graphite (HOPG) resulted in a direct visualization of PAT on a surface and revealed an interlayer spacing of 20 Å.[40] The authors attributed the shorter interchain distance to the orientation of the 3-dodecylthiophene units on the HOPG, which forces interdigitation of the side chains to occur. In comparison with other X-ray diffraction measurements, 30.5 Å agrees very well with data obtained for RR 3-dodecylthiophene.[9,36,38]

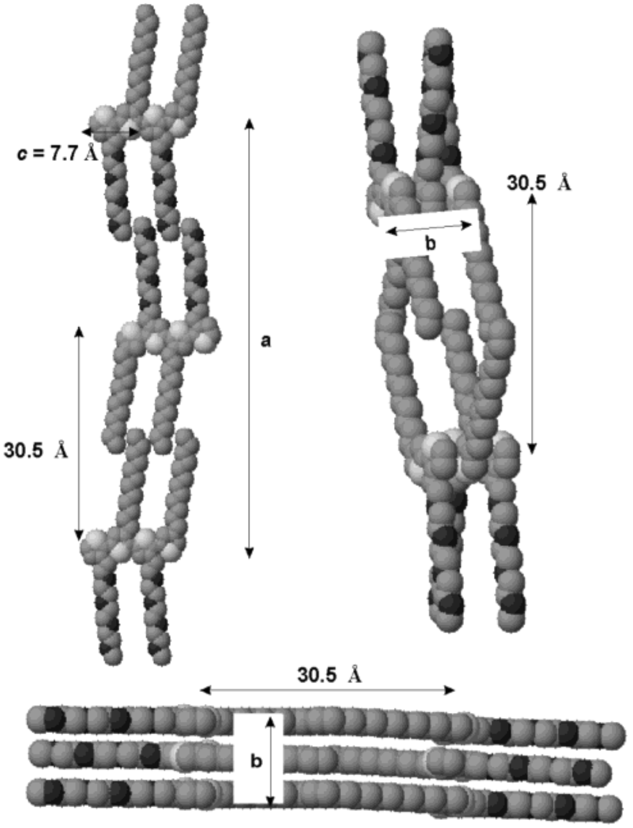

Figure 7. Schematic representation of the orientation of amphiphilic polythiophene as derived from the X-ray diffraction data. Space-filling model displays oligothiophenes: black: oxygen; light gray: sulfur; gray: carbon.

The diffraction peak of the bithiophene repeat unit (*c*-axis) at 11.4° (7.7 Å (001)) is clearly visible and corresponds well to the literature.[23,36,39] The spacing between the π-stacked polythiophene chains (*b*-axis) is expected to be around 3.8 Å ($\sim$2 Å = 23.1°)[20,36,38] but could not be detected due to the experimental setup.

To evaluate the thermotropic transitions that were obtained by DSC, we performed X-ray diffraction on an as-cast film of RR DTOT-PT (hex) at 25 °C, above both transitions of side-chain melting at 80 °C, above the backbone melting transition at 140 °C, and again after cooling to 90 °C (Figure 6). Upon increasing the temperature above the melting temperature of the side chains, the diffraction peak assigned to the interlayer *d*-spacing along the *a*-axis (30.5 Å) has disappeared, suggesting a transition to a disordered phase. The diffraction peak at 7.7 Å (11.4°, bithiophene repeat unit) remains at all temperatures, suggesting that there is still a high degree of chain alignment in the film. This diffraction peak might arise from high molecular weight fractions that require a higher temperature to melt. Subsequent cooling to 90 °C results in the reversible formation of layered thiophene chains and is consistent with DSC data.

Besides X-ray diffraction, optical microscopy indicates that a high degree of chain alignment is still present in the film. Increasing the temperature to 90 °C did not result in thermochromic behavior of the DTOT-PT film. Optical microscopy of a drop-cast solution of 1wt % RR DTOT-PT (hex) in chloroform visualized the red, solid structure at room temperature. At 90 °C the film behaves as a waxy solid, due to melting of the side chains and above 140 °C an isotropic melt is obtained.

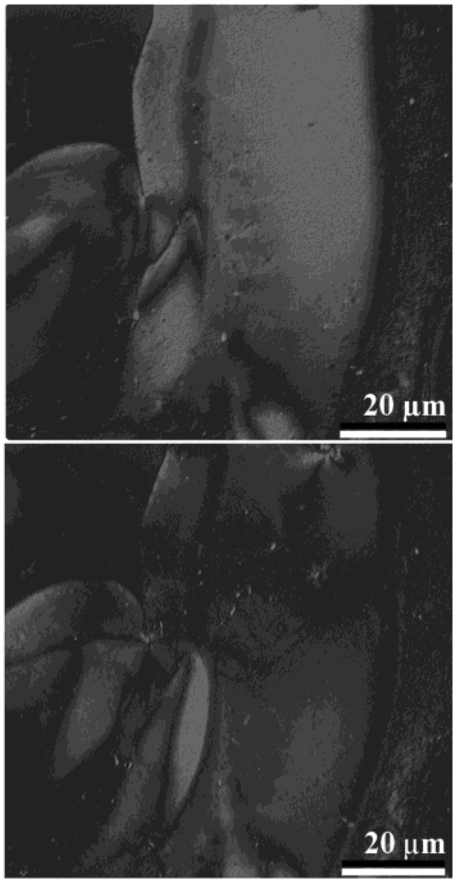

Figure 8. Optical microscopy (with crossed-polarizers) images of the liquid-crystalline phase of the regioregular, amphiphilic polythiophene DTOT-PT (hex) (top). The birefringence was visualized by rotating the sample by 45° (bottom).

After slowly cooling the sample (2 °C/min) from 200 to 20 °C, a crystalline phase was observed below 70 °C. The crystalline phase showed a clear birefringence (Figure 8) and proved to be stable up to 110 °C. Annealing of this film at 100 °C for several days increased the molecular packing and resulted in larger crystalline domains. Thus, optical microscopy (with crossed polarizers) confirms that a liquid-crystalline phase exists between the melting temperature of the side chains and the melting temperature of the polythiophene backbone, as previously measured with X-ray diffraction and DSC.

As cast from chloroform, the amphiphilic, RR PTs crystallize in small domains due to the rapid evaporation of chloroform. These domains are hardly visible with optical microscopy. Upon slow cooling from the isotropic melt, larger crystalline domains may form, because the PT chains can rearrange themselves during this process.

Crystallization, imaged by transmission electron microscopy (TEM), from chloroform solution produces triangular crystals of 0.5−1 μm (Figure 9A) and needles as well (Figure 9B). The thinnest needles have a diameter of the order of 10 nm; the edge of the deposit from which the needles originate shows triangular features as well.

Electron diffraction studies on the triangular crystals and needles revealed that the orientation of the polythiophene backbone is parallel to the substrate in the case of the triangular crystals and perpendicular to the substrate in the needles. Electron diffraction of the

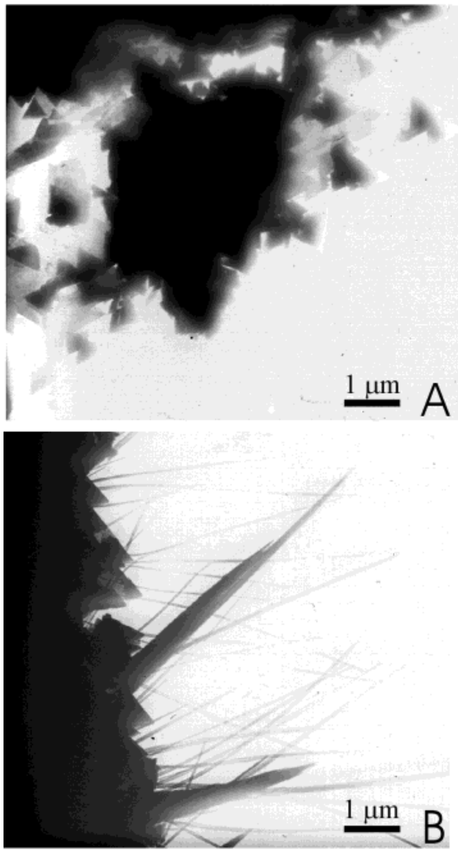

Figure 9. Transmission electron micrographs of RR DTOT-PT (hex) crystallized from chloroform solution. Both triangular crystals (A) and needles (B) are found.

needles resulted in a typical pattern that is commonly observed for polyethylene, which can be attributed to diffraction from the sublattice of the alkyl side chains. Electron diffraction of the triangles demonstrated a diffraction pattern related to the π-stacking spacing of the polythiophene backbone (*b*-axis).

This kind of amphiphilic, regioregular PTs exhibits the "ideal" structure for processing by LB techniques, and the high stereoregularity of the thiophene backbone ensures the high degree of conjugation that is essential for electrical and optical properties of devices.[18,19] Especially, field-effect transistors can benefit from oriented microcrystalline PATs[13] synthesized with regiochemical control, as was recently demonstrated by Sirringhaus et al.[16] and by Schön et al.[15]

Conclusion

The design, synthesis, and characterization of amphiphilic, regioregular polythiophenes consisting of an amphiphilic bithiophene repeat unit are described. When polymerized via a Stille coupling of the bifunctional dimer, the resulting amphiphilic polythiophene proved to consist of mainly head-to-tail coupled bithiophene repeat units, whereas the polymerization of the amphiphilic dimer with $FeCl_3$ resulted in a regioirregular polythiophene. The molecular weights of these polythiophenes were determined by means of standard GPC-LS in two different solvents, MALDI−TOF mass spectroscopy and light scattering (with measured d*n*/d*c*). Spreading a monolayer of the amphiphilic polythiophenes onto the water subphase of a Langmuir trough resulted in very stable films that could easily be compressed. The spread films were transferable (Langmuir−Blodgett) to hydrophilic substrates with a transfer ratio of nearly unity and the formation of multilayers proved to be possible. Mixed solutions of poly(ethylene glycol) and amphiphilic polythiophene resulted in a phase-separated monolayer that consisted of threads of polythiophene with dimensions comparable to the molecular length scale dispersed in a matrix of poly(ethylene glycol). Under specific conditions (composition and surface pressure), these threads form a continuous path of semiconducting polymer in an insulating matrix. In the bulk, condensed state, three thermotropic transitions were identified for the regioregular, amphiphilic polythiophenes, namely, melting of the tetraethylene glycol side chains (∼5 °C), melting of the dodecyl side chains (∼55 °C), and melting of the polythiophene backbone (∼120 °C). These transitions were determined and identified by means of DSC, optical microscopy, and X-ray diffraction.

Acknowledgment. We thank the Dutch Science Organization, the physics division (FOM), and the chemistry division (NWO−CW) for financial support. Furthermore, we thank J. Vorenkamp for assistance in GPC-LS, G. O. R. Alberda van Ekenstein for assistance in optical microscopy and DSC, J. Baas for assistance in X-ray diffraction, and N. Ouali for some preliminary investigations.

Supporting Information Available: The synthesis and analysis of all monomers and precursors are described in detail. This material is available free of charge via the Internet at http://pubs.acs.org.

References and Notes

(1) Yamamoto, T.; Sanechika, A.; Yamamoto, A. *J. Polym. Sci., Polym. Lett. Ed.* **1980**, *18*, 9−12.
(2) Lin, J. W. P.; Dudek, L. P. *J. Polym. Sci., Polym. Chem. Ed.* **1980**, *18*, 2869−2873.
(3) Yamamoto, T.; Sanechika, K. *Chem. Ind. (London)* **1982**, 301−302.
(4) Yamamoto, T.; Sanechika, K.; Yamamoto, A. *Bull. Chem. Soc. Jpn.* **1983**, *56*, 1497−1502.
(5) Jen, K. Y.; Oboodi, R.; Elsenbaumer, R. L. *Polym. Mater. Sci. Eng.* **1985**, *53*, 79−83.
(6) McCullough, R. D.; Lowe, R. D.; Jayaraman, M.; Anderson, D. L. *J. Org. Chem.* **1993**, *58*, 904−912.
(7) McCullough, R. D.; Lowe, R. D. *J. Chem. Soc., Chem. Commun.* **1992**, 70−72.
(8) Chen, T.-A.; Rieke, R. D. *Synth. Met.* **1993**, *60*, 175−177.
(9) Chen, T.-A.; Wu, X.; Rieke, R. D. *J. Am. Chem. Soc.* **1995**, *117*, 233−244.
(10) McCullough, R. D.; Williams, S. P.; Tristram-Nagle, S.; Jayaraman, M.; Ewbank, P. C.; Miller, L. *Synth. Met.* **1995**, *69*, 279−282.
(11) Österbacka, R.; An, C. P.; Jiang, X. M.; Vardeny, Z. V. *Science* **2000**, *287*, 839−842.
(12) Österbacka, R.; An, C. P.; Jiang, X. M.; Vardeny, Z. V. *Synth. Met.* **2001**, *116*, 317−320.
(13) Bao, Z.; Dodabalapur, A.; Lovinger, A. J. *Appl. Phys. Lett.* **1996**, *69*, 4108−4110.
(14) Sirringhaus, H.; Tessler, N.; Friend, R. H. *Science* **1998**, *280*, 1741−1744.
(15) Schön, J. H.; Dodabalapur, A.; Bao, Z.; Kloc, Ch.; Schenker, O.; Batlogg, B. *Nature (London)* **2001**, *410*, 189−191.
(16) Sirringhaus, H.; Brown, P. J.; Friend, R. H.; Nielsen, M. M.; Bechgaard, K.; Langeveld-Voss, B. M. W.; Spiering, A. J. H.; Janssen, R. A. J.; Meijer, E. W.; Herwig, P.; de Leeuw, D. M. *Nature (London)* **1999**, *401*, 685−688.
(17) Bjørnholm, T.; Greve, D. R.; Geisler, T.; Petersen, J. C.; Jayaraman, M.; McCullough, R. D. *Adv. Mater.* **1996**, *8*, 920−923.
(18) Xu, G.; Bao, Z.; Groves, J. T. *Langmuir* **2000**, *16*, 1834−1841.

(19) Bjørnholm, T.; Greve, D. R.; Reitzel, N.; Hassenkam, T.; Kjaer, K.; Howes, P. B.; Larsen, N. B.; Bøgelund, J.; Jayaraman, M.; Ewbank, P. C.; McCullough, R. D. *J. Am. Chem. Soc.* **1998**, *120*, 7643−7644.

(20) Reitzel, N.; Greve, D. R.; Kjaer, K.; Howes, P. B.; Jayaraman, M.; Savoy, S.; McCullough, R. D.; McDevitt, J. T.; Bjørnholm, T. *J. Am. Chem. Soc.* **2000**, *122*, 5788−5800.

(21) Hassenkam, T.; Greve, D. R.; Bjørnholm, T. *Adv. Mater.* **2001**, *13*, 631−634.

(22) Wu, A. P.; Kakimoto, M. A. *Adv. Mater.* **1995**, *7*, 812−814.

(23) Greve, D. R.; Reitzel, N.; Hassenkam, T.; Bøgelund, J.; Kjaer, K.; Howes, P. B.; Larsen, N. B.; Jayaraman, M.; McCullough, R. D.; Bjørnholm, T. *Synth. Met.* **1999**, *102*, 1502−1505.

(24) Qiao, X.; Wang, X.; Mo, Z. *Synth. Met.* **2001**, *118*, 89−95.

(25) McCullough, R. D.; Ewbank, P. C.; Loewe, R. S. *J. Am. Chem. Soc.* **1997**, *119*, 633−634.

(26) Räder, H. J.; Spickermann, J.; Kreyenschmidt, M.; Müllen, K. *Macromol. Chem. Phys.* **1996**, *197*, 3285−3296.

(27) Holdcroft, S. *J. Polym. Sci., Part B: Polym. Phys.* **1991**, *29*, 1585−1588.

(28) Montaude, G.; Montaude, M. S.; Puglisi, C.; Samperi, F. *Rapid Commun. Mass Spectrom.* **1995**, *9*, 453−460.

(29) Liu, J.; Loewe, R. S.; McCullough, R. D. *Macromolecules* **1999**, *32*, 5777−5785.

(30) Bjørnholm, T.; Hassenkam, T.; Greve, D. R.; McCullough, R. D.; Jayaraman, M.; Savoy, S. M.; Jones, C. E.; McDevitt, J. T. *Adv. Mater.* **1999**, *11*, 1218−1221.

(31) Cao, Y.; Smith, P.; Heeger, A. J. *Synth. Met.* **1992**, *48*, 91−97.

(32) Cao, Y.; Treacy, G. M.; Smith, P.; Heeger, A. J. *Appl. Phys. Lett.* **1992**, *60*, 2711−2713.

(33) Yang, C. Y.; Cao, Y.; Smith, P.; Heeger, A. J. *Synth. Met.* **1993**, *53*, 293−301.

(34) Yu, L.; Bao, Z. *Adv. Mater.* **1994**, *6*, 156−159.

(35) Poser, S.; Fischer, H.; Arnold, M. *Prog. Polym. Sci.* **1998**, *23*, 1337−1379.

(36) Prosa, T. J.; Winokur, M. J.; Moulton, J.; Smith, P.; Heeger, A. J. *Macromolecules* **1992**, *25*, 4364−4372.

(37) Gill, R. E.; Meetsma, A.; Hadziioannou, G. *Adv. Mater.* **1996**, *8*, 212−214.

(38) Chen, S.-A.; Ni, J.-M. *Macromolecules* **1992**, *25*, 6081−6089.

(39) Prosa, T. J.; Winokur, M. J.; McCullough, R. D. *Macromolecules* **1996**, *29*, 3654−3656.

(40) Mena-Osteritz, E.; Meyer, A.; Langeveld-Voss, B. M. W.; Janssen, R. A. J.; Meijer, E. W.; Bäuerle, P. *Angew. Chem., Int. Ed.* **2000**, *39*, 2680−2684.

MA011591W